JOC The Journal of Organic Chemistry

Article

pubs.acs.org/joc

Dehalogenation of Arenes via S_N2 Reactions at Bromine: Competition with Nucleophilic Aromatic Substitution.

Scott Gronert,*[†] John M. Garver,[‡] Charles M. Nichols,[‡] Benjamin B. Worker,[‡] and Veronica M. Bierbaum*[‡]

[†]Department of Chemistry, Virginia Commonwealth University, 1001 W. Main Street, Richmond, Virginia 23284-2006, United States

[‡]Department of Chemistry and Biochemistry, University of Colorado, 215 UCB, Boulder, Colorado 80309-0215, United States

Supporting Information

ABSTRACT: The gas-phase reactions of carbon- and nitrogen-centered nucleophiles with polyfluorobromobenzenes were examined in a selected-ion flow tube (SIFT) and modeled computationally at the MP2/6-31+G(d,p)//MP2/6-31+G(d) level. In the gas-phase experiments, rate constants and branching ratios were determined. The carbon nucleophiles produce expected nucleophilic aromatic substitution (S_NAr) and proton transfer products along with unexpected products that result from S_N2 reactions at the bromine center (polyfluorophenide leaving group). With nitrogen nucleophiles, the S_N2 at bromine channel is suppressed. In the S_NAr channels, the "element effect" is observed, and fluoride loss competes with bromide loss. The computational modeling indicates that all the substitution barriers are well below the entrance channel and that entropy and dynamics effects control the product distributions.

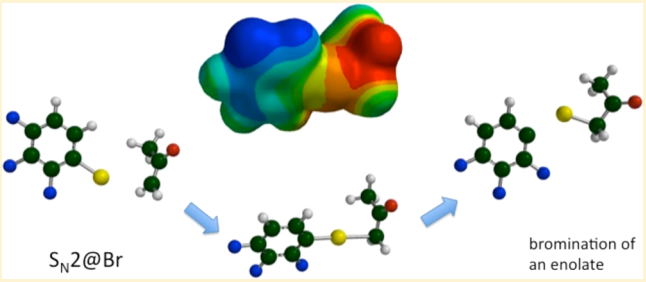

INTRODUCTION

When arenes are substituted with strong electron-withdrawing groups, nucleophilic aromatic substitution becomes a viable pathway and offers the ability to manipulate substituents on the arene. This is a well-established reaction that has been widely studied in the condensed phase[1−4] and the gas phase.[5−15] Another consequence of adding strong electron-withdrawing groups to an arene is that it converts the aryl moiety into a good leaving group and opens the door to S_N2 reactions on a halogen substituent (generally bromine or iodine). This represents a novel dehalogenation mechanism for arenes, and although known,[16,17] it has not been explored in great depth. Bunnett and Bolton provided several early examples employing carbon nucleophiles,[18−20] and there has been more recent work with sulfur nucleophiles.[21] The general reaction process is common in organometallic systems, but is typically classified as a metal/halogen exchange. S_N2 reactions at halogens have also been seen in saturated systems in the condensed phase.[22−24] There are examples of S_N2 reactions at halogen centers in the gas phase with saturated systems, but they are limited and do not offer the breadth of reactivity seen in aryl systems.[25−32] Here, we present a gas-phase study focused on the reaction of carbon and nitrogen nucleophiles with polyfluorobromobenzenes. The reactions produce a broad set of products, including nucleophilic substitutions at bromine centers, and suggest a delicate balance in the factors that determine the preferred leaving group (bromide vs fluoride) in S_NAr reactions. Moreover, the data highlight a sharp shift in product distributions from previous work employing oxygen-centered nucleophiles.[7]

The reactions of nucleophiles with activated haloarenes present an extremely broad set of mechanistic possibilities. The likely reaction paths are outlined in Scheme 1. They include proton transfer, S_NAr with loss of bromide, S_NAr with loss of fluoride, and S_N2 on bromine (S_N2@Br). The S_NAr reactions can proceed through concerted or stepwise mechanisms where

Scheme 1

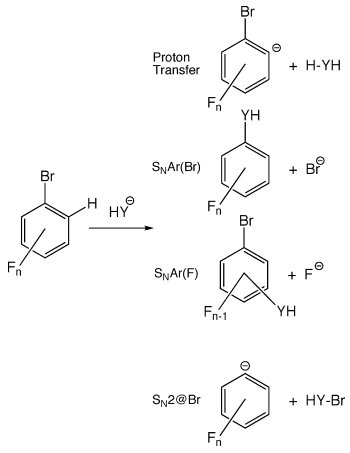

Received: September 3, 2014
Published: October 20, 2014

the Meisenheimer structure is either a stable complex or a transition state. When multiple leaving groups are available, interesting patterns in regiochemistry have been observed in S_NAr reactions, with poor leaving groups sometimes outcompeting better leaving groups on the arene. This phenomenon has been referred to as the "element effect".[33−35]

Previous gas-phase studies have also highlighted competing and secondary processes in these systems.[11,12,36] Less has been reported on the S_N2@Br reactions of aryl bromides,[37] but there is clear evidence for the process in the condensed phase for polyhalogenated systems.[16,21] In addition, computational work has been completed on model S_N2@Br reactions in alkyl halides.[38−40]

Reaction Systems. The focus of this study is nucleophilic aromatic substitution reactions using carbon- and nitrogen-centered nucleophiles. In the gas phase, there is a delicate balance in choosing nucleophiles that are reactive enough to allow S_NAr and S_N2@Br processes, but not so basic as to allow proton transfer to dominate the reaction channels. From a survey of potential nucleophiles, it became clear that anionic nucleophiles with proton affinities near 360−370 kcal/mol would be the best fit for the substrates in the study (Scheme 2).

Scheme 2

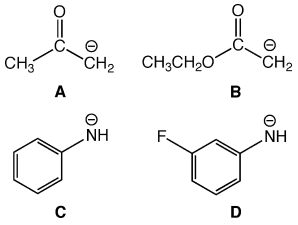

Acetone enolate (**A**, PA = 369 kcal/mol)[41] and anilide (**C**, PA = 366 kcal/mol) fit this criterion and were used most extensively in the study, but data are also provided for ethyl acetate enolate (**B**, PA = 369 kcal/mol) and 3-fluoroanilide (**D**, PA = 361 kcal/mol). The accuracy of the reported PA value for the ethyl acetate enolate is a concern because it is essentially the same as for the acetone enolate. Esters tend to be less acidic than ketones in the condensed phase, and this trend is also seen in computed values. At the G3MP2 level, the PAs of **A** and **B** are 369.6 and 374.1 kcal/mol, respectively. The proton transfer behavior in the present work also suggests that **B** is more basic than **A**. For the purposes of this study, we will interpret the results with the assumption that **B** is about 4 kcal/mol more basic than **A**.

For substrates, a series of polyfluorobromobenzenes has been employed. An initial survey of substrates indicated that a minimum of two fluorines is necessary to activate the arene for S_NAr reactions with the nucleophiles in this study. The substrates are shown in Scheme 3. The computed proton affinities of their most stable conjugate bases are listed in Table 1 and range from 356 to 366 kcal/mol (computed data for the less stable conjugate bases are also listed in the Supporting Information). The arenes with the most fluorines tend to be the most acidic, but there are exceptions to the trend. For example, 2,3,4-trifluorobromobenzene (**IV**) is 3 kcal/mol less acidic than 2,4-difluorobromobenzene (**VII**) and is 9 kcal/mol less acidic than an isomer, 2,4,5-trifluorobromobenzene (**V**). In a comparison of the acidities of these arenes to the nucleophiles, the enolates should be capable of deprotonating all of the arenes (aside from **I**, which lacks a proton). With the anilides, the proton transfer processes are less exothermic or, in some instances, endothermic.

Scheme 3

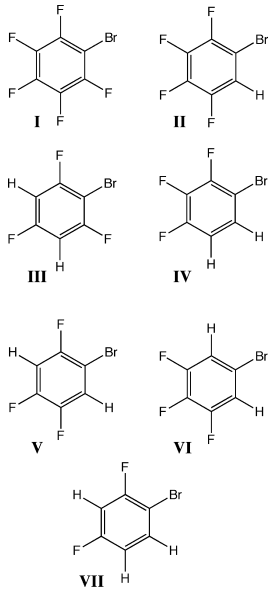

Table 1. Proton Affinities of Most Stable Conjugate Bases of the Arenes and the Proton Affinities of the Substrates' Debromination Products

species	PA conjugate base	location[b]	PA debromination product
I			355
II	356	C-6	368
III	360	C-3	367
IV	366	C-5	374
V	357	C-6	375
VI	361	C-2	382
VII	363	C-3	380

[a]kcal/mol computed at the MP2/6-31+G(d,p)//MP2/6-31+G(d) level. [b]Most acidic sites in substrates **II**−**VII**.

In all the reactions in Scheme 1, it is expected that the barriers will be sensitive to the number of fluorine electron-withdrawing groups on the arene. However, the number of fluorines will only have a marked effect on the exothermicities of the proton transfer and S_N2@Br reactions because only in these processes is the charge retained on the arene. Of course the basicity of the nucleophile will impact the barriers and exothermicities of all these reactions.

METHODS

Mass Spectrometry. The experimental work was conducted at the University of Colorado using a flowing afterglow-selected ion flow tube (FA-SIFT) instrument that has been previously described.[42,43] Ions were formed in a flowing afterglow ion source, and then, a quadrupole mass filter was used for mass selection prior to injection into the reaction flow tube. Hydroxide was prepared by electron ionization (70 eV) of methane and nitrous oxide (2:1 ratio), and amide ion was prepared by election ionization of ammonia. The ionic reagents in the study were generated by proton abstraction from neutral precursors by HO^- or NH_2^-. Injected ions were entrained in a flow of helium (200 std $cm^3\ s^{-1}$, 0.5 Torr) and thermalized to ambient temperature prior to reactions with the neutral reagents, which were added through multiple inlets along the length of the reaction flow tube. Ionic reactants and products were analyzed in the detection region using a triple-quadrupole mass filter and an electron multiplier.

dx.doi.org/10.1021/jo502039h | J. Org. Chem. 2014, 79, 11020−11028

The reactions were carried out under pseudo-first-order conditions, and the reported branching ratios and reaction rate coefficients are the averages of at least three individual measurements. The reported reaction efficiencies are the experimental rate constant divided by the calculated collision rate constant. Collision rate constants were calculated from parametrized trajectory collision rate theory.[44] The necessary polarizabilities were calculated from the known refractive indices of the substrates, and the dipole moments were taken from MP2/6-31+G(d,p)//MP2/6-31+G(d) level calculations on the substrates. Error bars in the rate constant measurements represent one standard deviation in the data; absolute uncertainties in these rate constant measurements are ±20%. Product branching fractions were determined by monitoring the complete product spectra at each of the seven inlets, and extrapolating the product fractions to zero time; this approach eliminates effects of secondary reaction and differential diffusion of the ions. The detector was tuned to minimize mass discrimination, and no further corrections were made in the analysis.

Materials. All compounds were obtained from commercial vendors (Sigma-Aldrich and TCI America) in the highest purity available. Helium buffer gas (99.995%) was purified by passage through a molecular sieve trap immersed in liquid nitrogen.

Computational Methods. Ab initio molecular orbital calculations were completed at the MP2/6-31+G(d,p)//MP2/6-31+G(d) level using the Gaussian 03 suite of programs.[45] Frequency calculations were completed at the HF/6-31+G(d) level and relative energies are corrected for zero-point vibrational energies at 0 K (scaled by 0.9135 at the HF level and 0.967 at the MP2 level).[46] In some cases, the stationary points could only be found at the MP2 level, and MP2 frequencies were used. The G3MP2 composite method was used for more accurate energy calculations of the proton affinities of acetone and ethyl acetate.

RESULTS

Pentafluorobromobenzene (I). This substrate is incapable of proton transfer reactions and is limited to S_NAr and S_N2@Br pathways. All of the nucleophiles give moderately fast reactions (efficiencies ∼50%) with this substrate (Table 2). Product distributions and partial rate constants are shown in Figures 1−3. In the S_NAr(F) process, the observed product is the result of addition with the loss of HF. The fluoride leaving group is sufficiently basic to deprotonate the addition product before departing the product complex (Scheme 4), presumably at the site of the original nucleophilic center (e.g., the nitrogen of the anilide nucleophile). This process is highly exothermic because the reaction adds a polyhalogenated phenyl group to that site and greatly enhances its acidity. The product ratios are very sensitive to the nature of the nucleophile, with the enolates giving mainly S_NAr(Br) and S_N2@Br reactions and the anilides giving mainly S_NAr(F) reactions.

Table 2. Rate Constants for the Reactions of Nucleophiles with Polyfluorobromobenzenes

nucleophile	substrate	k^a	SD[a]	efficiency
acetone enolate (**A**)	**I**	9.3	0.1	52%
	II	10.5	0.2	55%
	III	7.2	0.3	44%
	IV	4.4	0.1	19%
	V	7.3	0.3	55%
	VII	1.0	0.1	6%
EtOAc enolate (**B**)	**I**	7.9	0.4	52%
	II	9.3	0.3	57%
	III	7.2	0.2	52%
anilide (**C**)	**I**	7.5	0.1	51%
	II	8.9	0.3	56%
	III	7.9	0.1	59%
	IV	5.8	0.7	29%
	V	7.6	0.3	68%
	VI	7.7	0.8	48%
	VII	6.7	0.1	45%
3-F anilide (**D**)	**I**	6.1	0.2	44%
	II	8.1	0.2	54%
	III	2.4	0.1	19%

[a]Units are 10^{-10} cm^3 molecule^{-1} s^{-1}. SD indicates standard deviation.

2,3,4,5-Tetrafluorophenyl Bromide (II). This substrate contains an acidic hydrogen (ΔH_{acid} = 356 kcal/mol) and gives the highest rate constants in the series. Proton transfer dominates the product distributions, particularly with the anilides, where it is the sole path. The preference for proton transfer is not surprising given that **II** is 5−18 kcal/mol more acidic than the nucleophiles in the study. With **A**, the other important channel is S_NAr(Br), which was also a significant pathway in **I**. With **B**, proton transfer dominates, but there is a significant amount of a product related to the S_N2@Br pathway. The initial phenide product is not observed in this S_N2@Br reaction to a significant extent (<1%), but instead, the product of a secondary deprotonation reaction occurs in the reaction complex, which leads to an overall exchange of an H for a Br on the nucleophile in the reaction process (Scheme 5). The bromination of the nucleophile enhances its acidity and makes the secondary reaction favorable.

Trifluorobromobenzenes (III−VI). The trifluorobromobenzenes each have two acidic hydrogens, and the substrates have ΔH_{acid} values that range from 357 to 366 kcal/mol (Table 1). The pattern in acidity indicates that there is a substantial preference to having halogens *ortho* to the charge site in the resulting anion. **IV** stands out from the set as being the least acidic because it is the only one where deprotonation must lead to an anion with a hydrogen *ortho* to the charge site. The difference in acidity is reflected in the observed rate constants, with **IV** reacting roughly 60% as fast as the other trifluorobromobenzenes, mainly due to a suppression of its proton transfer channel. With the enolates, there is more diversity in the product channels than with the anilides. **III** gives mainly deprotonation with the enolates, but also significant amounts of S_NAr(Br), S_NAr(F), and S_N2@Br reactions. In the S_N2@Br reaction of **A** with **III**, the initial phenide product is not observed, but instead, the product of the secondary deprotonation reaction is observed (Scheme 5). With **A**, the production of the trifluorophenide from **III** is slightly endothermic (by 1 kcal/mol), and the secondary proton transfer is needed to make the process exothermic (by 11 kcal/mol). Similar data were observed with **B**, although the S_N2@Br reaction produced a small yield of the free phenide because it is exothermic with the more basic nucleophile. **IV** gives nearly equal amounts of S_NAr(Br), S_NAr(F), and proton transfer reactions as well as a small amount of adduct formation with **A**. The absence of the S_N2@Br reaction can be attributed to the relatively high basicity of the phenide leaving group (7 kcal/mol higher than the phenide from **III**, see Table 1), which makes the S_N2@Br process more endothermic (10 kcal/mol). **V** is the most acidic of this group, and only proton transfer is observed with **A**. With **C**, **III** and **V** mainly give proton transfer, with only a trivial yield of a S_NAr(F) product. **IV** gives mainly S_NAr(F), but also S_NAr(Br) and proton transfer pathways. The reaction of **D** with **III** gives mainly proton transfer, but also some S_NAr(F).

dx.doi.org/10.1021/jo502039h | J. Org. Chem. 2014, 79, 11020−11028

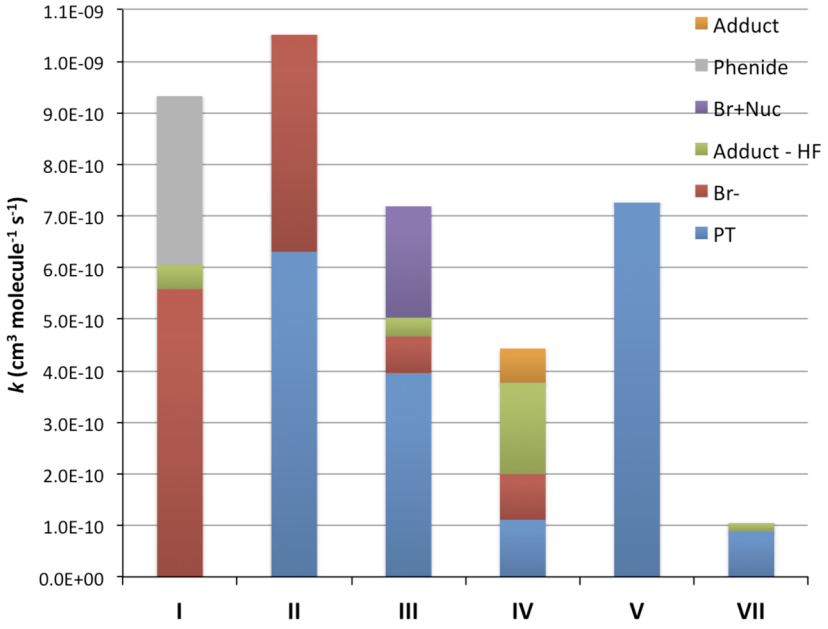

Figure 1. Partial rate constants for the reactions of **A** with polyfluorobromobenzenes (cm^3 $molecule^{-1}$ s^{-1}). PT refers to proton transfer, and phenide is the product of the S_N2@Br reaction. Br + Nuc refers to products in Scheme 5, and Adduct − HF refers to products in Scheme 4.

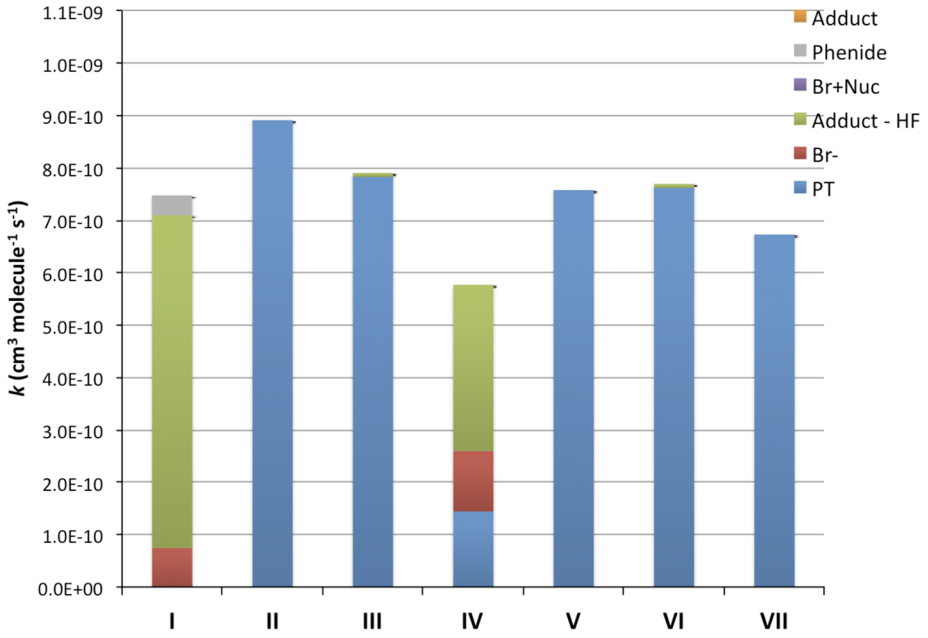

Figure 2. Partial rate constants for the reactions of **C** with polyfluorobromobenzenes (cm^3 $molecule^{-1}$ s^{-1}). PT refers to proton transfer, and phenide is the product of the S_N2@Br reaction. Not all listed product channels are observed. Br + Nuc refers to products in Scheme 5, and Adduct − HF refers to products in Scheme 4.

2,4-Difluorobromobenzene (VII). This substrate has an acidity comparable to **IV**. Interestingly, when **VII** is reacted with **A**, it exhibits a similar proton transfer rate constant to **IV** (Figure 1). However, the other reactions are greatly attenuated due to the reduced number of activating groups on the ring. Only a small amount of product from an $S_NAr(F)$ pathway competes with proton transfer. With **C**, a relatively fast proton transfer is observed as the sole reaction pathway. Despite its lower PA, the greater localization of **C** leads to greater kinetic basicity and a higher proton transfer rate constant than acetone enolate.

Computational Modeling. Substrate **IV** gave the widest range of reactivity so it was chosen for computational modeling at the MP2/6-31+G(d,p)//MP2/6-31+G(d) level with acetone enolate and anilide (Table 3). The enolate could be treated as a carbon or oxygen nucleophile. In previous work, Nibbering[47] has shown that enolates give distinctive products in their reactions with hexafluorobenzene that distinguish between C- and O-arylation. As a carbon nucleophile, addition with loss of HF is observed with enolates, but as an oxygen nucleophile, pentafluorophenoxide is observed, resulting from a secondary elimination process. For **A**, they found that 75% of the reactions corresponded to C-arylation. Experimentally, we only

dx.doi.org/10.1021/jo502039h | J. Org. Chem. 2014, 79, 11020−11028

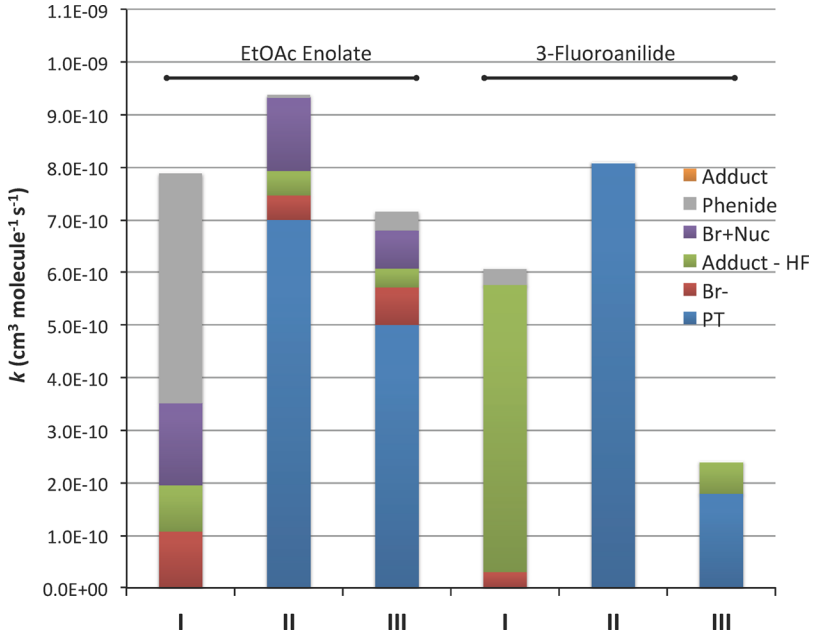

Figure 3. Partial rate constants for the reactions of ethyl acetate enolate (**B**) and 3-fluoroanilide (**D**) with **I**–**III** (cm^3 $molecule^{-1}$ s^{-1}). PT refers to proton transfer, and phenide is the product of the S_N2@Br reaction. Not all listed product channels are observed. Br + Nuc refers to products in Scheme 5, and Adduct − HF refers to products in Scheme 4.

Scheme 4

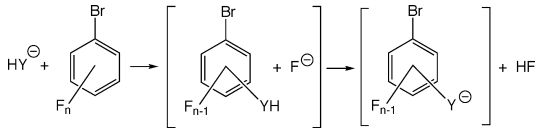

Scheme 5

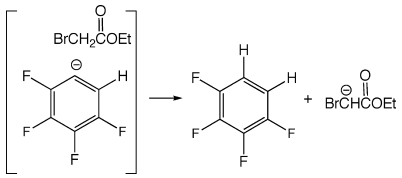

Table 3. Computed Transition State Energies for Reactions with Substrate IV

nucleophile	pathway	TS energy[a]	products[a]
acetone enolate (**A**)	S_N2@Br	−15.7	10.0 (−11)
	S_NAr(F2)	−16.3	
	S_NAr(F3)	−15.3	−32.3 (−50.8)
	S_NAr(F4)	−12.7	
	S_NAr(Br)	−13.4	−53.4
	PT	−8.1	−4.0
anilide (**C**)	S_N2@Br	−21.6	31.3 (0)
	S_NAr(F2)	−24.9	−24.8 (−50.2)
	S_NAr(F3)	−24.5	
	S_NAr(F4)	−17.3	
	S_NAr(Br)	−16.8	−47.8
	PT	−18.3	−1.6

[a]kcal/mol computed at the MP2/6-31+G(d,p)//MP2/6-31+G(d) level. See Methods section for details. Values in parentheses refer to secondary proton transfer products.

saw evidence of a phenoxide product with **I** (<5%), and a sample calculation of the S_NAr barrier for bromide loss with **IV** had a significantly higher barrier (by 5 kcal/mol) with oxygen as the nucleophilic site. For these reasons, we have limited our computational analysis to the reactions of the enolate as a carbon nucleophile. However, it is possible that some products from oxygen arylation are formed in the experiments.[47]

For representative paths, the energies of the products were computed. The S_NAr reactions of **A** and **C** with **IV** are extremely favorable with the bromide loss channels being exothermic by ∼50 kcal/mol and the fluoride loss channels being exothermic by ∼25 kcal/mol. When the secondary proton transfer is included in the process (i.e., addition −HF product), the S_NAr(F) channels are nearly as exothermic as the S_NAr(Br) channels (Scheme 4). The substitution products are reasonably acidic, with PAs around 340 kcal/mol, which allows the secondary proton transfer to add 30 kcal/mol of exothermicity to the reaction. The S_N2@Br channels are endothermic with **IV**, in part because the leaving group (2,3,4-trifluorophenide, PA = 374 kcal/mol) is more basic than the nucleophiles. The S_N2@Br reaction with **C** is much less favorable because the product has a weak N−Br bond. As with the S_NAr processes, very favorable secondary proton transfer reactions are possible and make the overall S_N2@Br processes thermoneutral or exothermic. By design, the simple proton transfer reactions are computed to be mildly exothermic in these systems.

Representative transition states for the four general processes with **A** as the nucleophile are shown in Figure 4. The S_NAr reactions exhibit extremely early transition states with little extension of the leaving group bond or rehybridization of the carbon at the site of attack. Surveys of the potential energy surface indicate that these are single-step processes without a Meisenheimer intermediate. Although not shown, the other S_NAr transition states for fluoride loss are similar in structure. The S_N2@Br process leads to an intermediate and proceeds through an addition/elimination pathway. The intermediate appears to be early on the reaction coordinate with the forming C−Br bond being considerably longer than the bond being

dx.doi.org/10.1021/jo502039h | J. Org. Chem. 2014, 79, 11020−11028

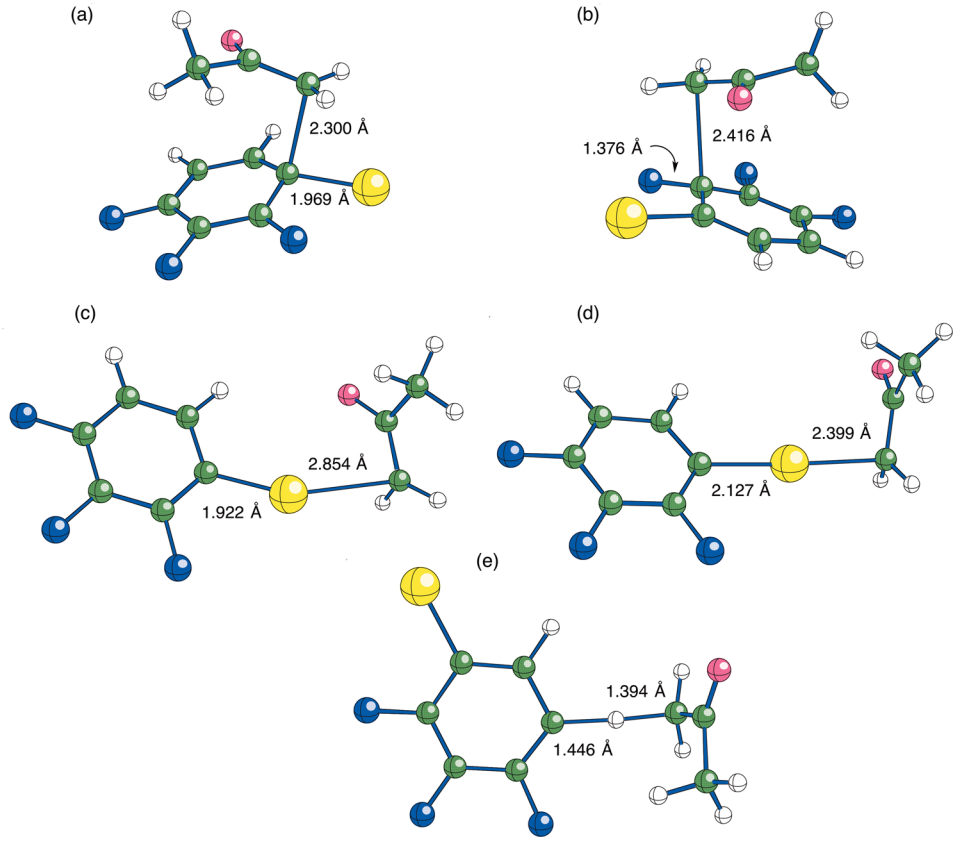

Figure 4. Stationary points in the reactions of **A** with **IV** at the MP2/6-31+G(d) level. (a) S_NAr with bromide loss transition state; (b) S_NAr with fluoride loss transition state (most stable pathway); (c) S_N2@Br transition state; (d) S_N2@Br intermediate; and (e) proton transfer transition state.

broken. Finally, the proton transfer transition state is late on the reaction coordinate with the breaking C−H distance being 0.05 Å longer than the forming bond distance despite this being an exothermic process. Each of the transition states and the intermediate lie below the entrance channel, particularly the S_NAr and S_N2@Br transition states, which are about 15 kcal/mol more stable than the reactants (Table 3).

The reactions with **C** are shown in Figure 5. Again the S_NAr transition states are early, extremely so in the reaction with loss of fluoride. The S_N2@Br process involves an intermediate, and it appears to be early on the reaction coordinate. Finally, the proton transfer transition state is slightly late, but to a lesser extent than was seen for the enolate. The S_NAr transition states and the S_N2@Br intermediate are well below the entrance channel and are lower in relative energy than those found for the acetone enolate reactions.

To gain a better understanding of the reaction pathways, the potential energy surfaces were scanned for the S_N2@Br processes. They scans were calculated by systematically fixing one of the bond lengths involved in the reaction coordinate and optimizing the other geometric parameters. The surfaces rise slightly from very stable ion/molecule complexes to transition states that lead to shallow wells for the intermediates. The surfaces then rise sharply to give the brominated nucleophiles and the debrominated phenide anions. As noted above, the processes are endothermic for the enolate and anilide nucleophiles with **IV** (by 10 and 31 kcal/mol, respectively); however, the reactions are overall exothermic or thermoneutral (by 11 and 0 kcal/mol, respectively) if they are coupled to the secondary proton transfer processes giving brominated nucleophiles as products (Scheme 5). For **IV**, the endothermicities of these reactions, rather than a kinetic barrier, suppress the S_N2@Br pathways.

DISCUSSION

The data in Table 2 and Figures 1−3 highlight the wide range of mechanisms that are possible in the reactions of highly activated arenes with nucleophiles, particularly carbon-centered nucleophiles. The systems produce three general competing processes: proton transfer, S_N2 at bromine, and nucleophilic aromatic substitution with either bromide or fluoride as the leaving group. Depending on the nucleophile/substrate combination, each of these processes can lead to the major or nearly major product. This reflects an unusually delicate balance between reaction pathways in a relatively simple system.

S_N2@Br Reactions. This pathway has not been observed previously in the gas-phase reactions of aryl bromides, but has been observed with alkyl bromides.[25−32] In the present study, it is most prominent with the carbon-centered nucleophiles and is an important process in their reactions with substrates **I** and **III**. The limited activity of the S_N2@Br process with the anilides is likely related to the formation of a weak N−Br bond in the process, which contributes to the endothermicity of the reactions. Because **I** offers the best S_N2@Br leaving group in this series, pentafluorophenide (Table 1), it is not surprising that the mechanism is most active with this substrate. There is no competition with proton transfer in this substrate so the reactivity is split between S_N2@Br and S_NAr reactions. The S_N2@Br channel is not seen in **II**, presumably because **II** gives a much less stable debromination product (13 kcal/mol more basic than the debromination product from **I**) and it has access

dx.doi.org/10.1021/jo502039h | J. Org. Chem. 2014, 79, 11020−11028

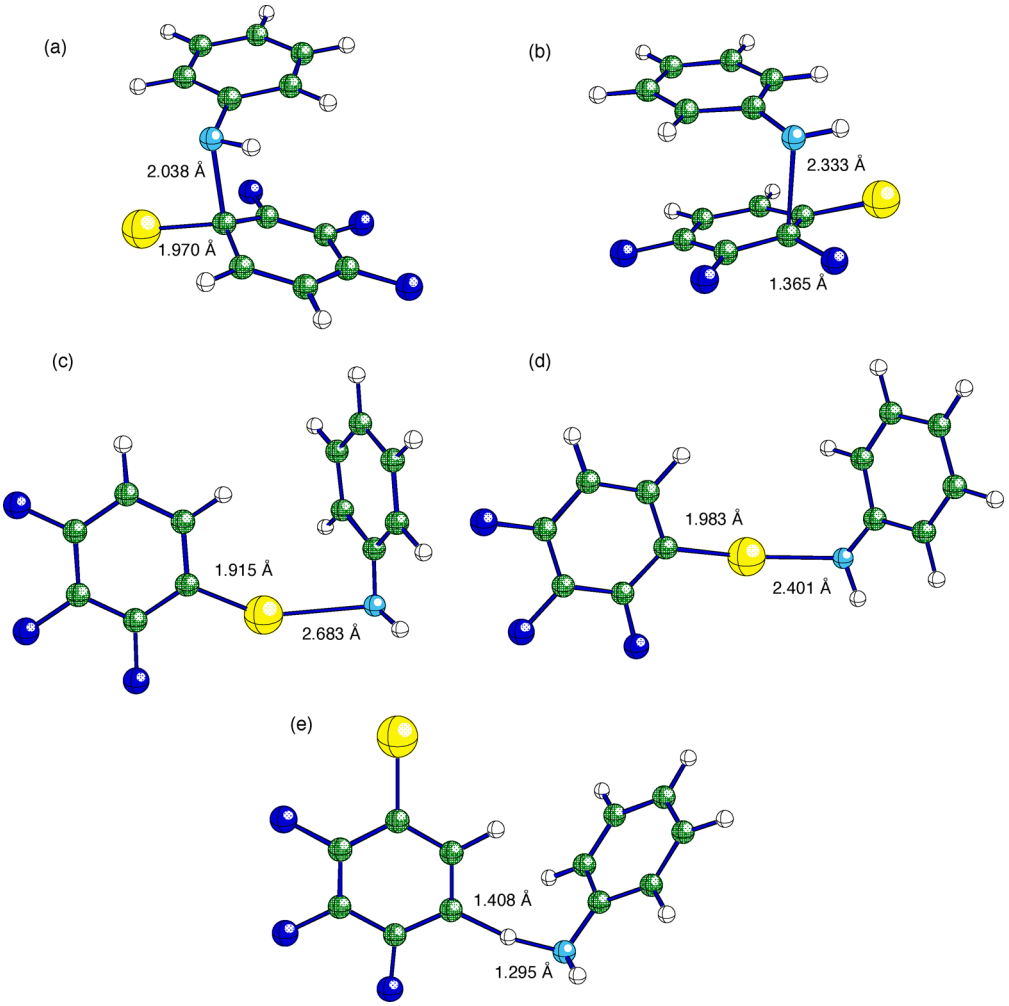

Figure 5. Stationary points in the reactions of **C** with **IV** at the MP2/6-31+G(d) level. (a) S_NAr with bromide loss transition state; (b) S_NAr with fluoride loss transition state (most stable pathway); (c) S_N2@Br transition state; (d) S_N2@Br intermediate; and (e) proton transfer transition state.

to a fast proton transfer channel. Surprisingly, only one of the trifluorobromobenzenes gives an S_N2@Br product with **A**. The preference for an S_N2@Br reaction in the trifluorobromobenzenes is clearly driven by the stability of the debromination product. Substrate **III** gives a debromination product, 2,4,6-trifluorophenide, that is 7 kcal/mol less basic than those from substrates **IV** and **V** (Table 1). This allows the S_N2@Br process to be nearly thermoneutral with **A**. Despite its stability, 2,4,6-trifluorophenide is considerably more basic than the S_N2@Br product, bromoacetone, and a secondary reaction in the product complex leads exclusively to deprotonated bromoacetone (Scheme 5), making the overall process significantly exothermic. Overall, the S_N2@Br process has a fairly limited scope in these arenes because factors that stabilize the leaving group also tend to activate the system for other processes, including entropically favorable proton transfers.

S_NAr Reactions. Nucleophilic aromatic substitution plays an important role in most of the reactions of the enolates and is the only process that effectively competes with proton transfer reactions with the anilide nucleophiles. A striking feature of this process is the delicate balance between bromide and fluoride as the leaving group. For **A**, bromide loss is favored for **I**, **II**, and **III**, but fluoride loss is preferred with **IV**. In contrast, fluoride loss is favored for **C** with **I** and **IV**, but more so with **I**. In all cases, bromide loss is much more favorable thermodynamically than fluoride loss. The appearance of a fluoride loss pathway in such systems has been referred to as the "element effect", and it appears to be driven by the greater polarization of C−F bonds and the resulting greater positive charge on that ring carbon.[34,35] Although well-established in the condensed phase, it is a striking result in gas-phase systems where the basicity difference between bromide and fluoride is increased (PA = 328 vs 371 kcal/mol). The present data suggest that the more localized nucleophile, **C**, tends to give more fluoride loss. This can be rationalized by the fact the localization of the anion's charge would enhance electrostatic interactions with the carbon centers bearing the greatest positive charge (i.e., C−F). In previous work with oxygen-centered, dianion nucleophiles we also saw a general preference for fluoride loss in trifluorobromobenzenes.[7] In sharp contrast, **I** gave exclusive bromide loss with the oxygen-centered, dianion nucleophiles whereas **C**, a nitrogen nucleophile, prefers fluoride loss from **I** by a wide margin. However, data from the dianion systems indicate that the release of internal electrostatic repulsion plays a role in the product distributions so direct comparisons between the singly and doubly charged systems are not wholly appropriate. Moreover, the oxygen nucleophile does not allow for the secondary proton transfer seen with the anilide anion. Overall, the factors controlling the pattern of fluoride versus bromide loss in these systems are not completely clear from the

dx.doi.org/10.1021/jo502039h | J. Org. Chem. 2014, 79, 11020−11028

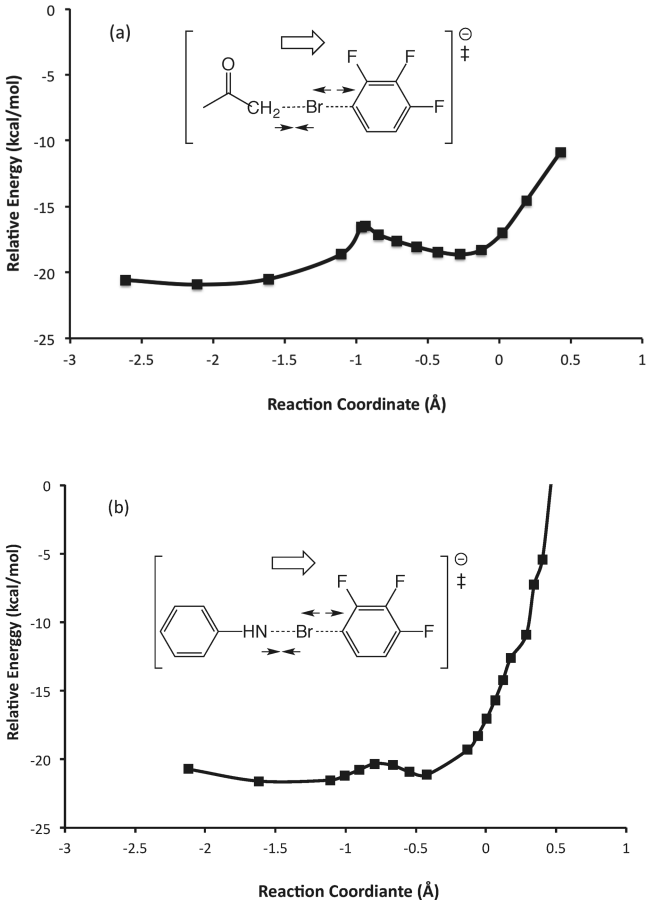

Figure 6. Potential energy scans for the S_N2@Br reactions of (a) **A** and (b) **C** with **IV**. The reaction coordinate is defined as the difference between the breaking C−Br and the forming Br−C or Br−N bond lengths. Negative values correspond to the approach of the nucleophile to **IV**. Energies and structures at the MP2/6-31+G(d) level. Arrows indicate key molecular motions along the reaction coordinate in the direction of the block arrow.

experimental results and are discussed below with the aid of computational data.

Computational Model. With substrate **IV** and **A**, the barriers for all the processes are below the energy of the entrance channel. The S_NAr processes have transition state energies ranging from −12.7 to −16.3 kcal/mol, with attack at carbon-2 (fluoride loss) having the most stable transition state. S_NAr with loss of bromide gives a transition state that is about 3 kcal/mol less favorable, but still well below the entrance channel at −13.4 kcal/mol. The S_N2@Br reaction proceeds through an addition/elimination process with a transition state that is 15.7 kcal/mol below the entrance channel, but the overall process is endothermic by 10 kcal/mol. These computed barriers are generally consistent with the mechanistic preferences observed in the experiments, but with barriers so far below the entrance channel, other factors related to the phase space available to the reaction pathways are expected to play a large role in the product distributions. This is clearly the case since the reaction of the enolate with **IV** gives roughly equal yields of products from pathways with transition state energies that vary from −8.1 (proton transfer) to −16.3 (S_NAr at C-2) kcal/mol.

With the **C** and **IV**, the calculations indicate a very strong preference for the S_NAr pathway with fluoride loss (favored by 8 kcal/mol over bromide loss). Proton transfer is computed to be competitive (transition state energy = −18.3 kcal/mol), whereas the S_N2@Br path is endothermic by over 30 kcal/mol. The S_NAr(F) reaction is the preferred pathway experimentally, but the significant yield of the S_NAr(Br) products observed experimentally is not consistent with the large difference in computed transition state energies. Here again it appears that factors other than barrier heights are controlling the product mixtures.

Finally, the most striking aspect of the kinetics is that despite having many paths with negative activation energies, the rate constants are well below the collision-controlled limit, and the efficiencies often dip below 50%. This is true even when there are pathways, such as proton transfer, that are not expected to produce entropic bottlenecks. With barriers located as much as 15 kcal/mol below the entrance channel, this immediately suggests nonstatistical reaction dynamics and the presence of nonproductive trajectories that do not explore the full potential energy surface of the encounter complex. These pathways could include additions to nonhalogenated carbons on the ring (except in **I**) or direct collisions with fluorine atoms on the ring. For **IV**, the S_N2@F reaction (at F-2) is predicted to have a barrier of 23.6 kcal/mol and could not lead to a successful reaction. With nonstatistical behavior, the computational analysis can provide a good picture of the potential energy surface and the relevant transition states, yet provide only general guidance in terms of the competition between channels. Unfortunately, these large systems are not amenable to trajectory studies or other analyses of the reaction dynamics.

■ CONCLUSIONS

These studies highlight the broad set of competing pathways in the reactions of nucleophiles with halogenated arenes. When carbon is the nucleophile, S_N2 reactions at bromine are observed and under the proper circumstances become significant product channels. These reactions proceed through addition/elimination pathways involving a hypervalent bromine intermediate. The study suggests that S_N2@Br reactions could potentially be further developed as a synthetic approach with the proper choice of nucleophile. These systems also produce S_NAr reactions, and as has been observed before, the stability of the leaving group does not determine the preferred pathway; in many examples, fluoride loss is preferred over bromide loss. With these arenes and nucleophiles, nucleophilic addition to the benzene π-system is strongly exothermic, independent of the *ipso* halogen. The overall trends suggest that factors related to the "element effect" are at play in the S_NAr reactions, but given the low barriers for the processes, entropic factors are critical in determining the product distribution.

■ ASSOCIATED CONTENT

Supporting Information

Full citation for ref 45 as well as Cartesian coordinates and energies for all species in the study. This material is available free of charge via the Internet at http://pubs.acs.org.

■ AUTHOR INFORMATION

Corresponding Authors

*E-mail: sgronert@vcu.edu.
*E-mail: Veronica.Bierbaum@Colorado.edu.

Notes

The authors declare no competing financial interest.

■ ACKNOWLEDGMENTS

S.G. acknowledges support from the National Science Foundation (CHE-1011771 and CHE-1300817). V.M.B. acknowledges support from the National Science Foundation (CHE-1300886).

■ REFERENCES

(1) Buncel, E.; Dust, J. M.; Terrier, F. *Chem. Rev.* **1995**, *95*, 2261.
(2) Bernasconi, C. F. *Acc. Chem. Res.* **1978**, *11*, 147.
(3) Miller, J. *Aromatic Nucleophilic Substitution*; Elsevier: Amsterdam, 1968.
(4) Bunnett, J. F.; Zahler, R. E. *Chem. Rev.* **1951**, *49*, 273.
(5) Chen, H.; Chen, H. W.; Cooks, R. G. *J. Am. Soc. Mass Spectrom.* **2004**, *15*, 998.
(6) Danikiewicz, W.; Bienkowski, T.; Kozlowska, D.; Zimnicka, M. *J. Am. Soc. Mass Spectrom.* **2007**, *18*, 1351.
(7) Eanes, A. D.; Noin, D. O.; Kebede, M. K.; Gronert, S. *J. Am. Soc. Mass Spectrom.* **2014**, *25*, 10.
(8) Fernandez, I.; Frenking, G.; Uggerud, E. *J. Org. Chem.* **2010**, *75*, 2971.
(9) Giroldo, T.; Xavier, L. A.; Riveros, J. M. *Angew. Chem., Int. Ed.* **2004**, *43*, 3588.
(10) Gluz, E. B.; Glukhovtsev, M. N.; Simkin, B. Y.; Minkin, V. I. *Zh. Org. Khim.* **1992**, *28*, 657.
(11) Gronert, S. *Chem. Rev.* **2001**, *101*, 329.
(12) Ingemann, S.; Nibbering, N. M. M.; Sullivan, S. A.; DePuy, C. H. *J. Am. Chem. Soc.* **1982**, *104*, 6520.
(13) Ingemann, S.; Nibbering, N. M. M. *Nouv. J. Chim.* **1984**, *8*, 299.
(14) Nibbering, N. M. M. *Mass Spectrom. Rev.* **2006**, *25*, 962.
(15) Vlasov, V. M. *J. Fluorine Chem.* **1993**, *61*, 193.
(16) Sazonov, P. K.; Artamkina, G. A.; Beletskaya, I. P. *Russ. Chem. Rev.* **2012**, *81*, 317.
(17) Zefirov, N. S.; Makhonkov, D. I. *Chem. Rev.* **1982**, *82*, 615.
(18) Bolton, R.; Moore, C.; Sandall, J. P. B. *J. Chem. Soc., Perkin Trans. 2* **1982**, 1593.
(19) Bolton, R.; Sandall, J. P. B. *J. Chem. Soc., Perkin Trans. 2* **1976**, 1545.
(20) Bunnett, J. F. *Acc. Chem. Res.* **1972**, *5*, 139.
(21) Banks, B.; Cargill, M. R.; Sandford, G.; Tadeusiak, A. J.; Westemeier, H.; Yufit, D. S.; Howard, J. A. K.; Kilickiran, P.; Nelles, G. *J. Fluorine Chem.* **2010**, *131*, 627.
(22) Li, X. Y.; Pan, H. Q.; Jiang, X. K. *Tetrahedron Lett.* **1984**, *25*, 4937.
(23) Li, X. Y.; Jiang, X. K.; Pan, H. Q.; Hu, J. S.; Fu, W. M. *Pure Appl. Chem.* **1987**, *59*, 1015.
(24) Li, X. Y.; Pan, H. Q.; Jiang, X. K.; Zhan, Z. Y. *Angew. Chem., Int. Ed. Engl.* **1985**, *24*, 871.
(25) Tanaka, K.; Mackay, G. I.; Payzant, J. D.; Bohme, D. K. *Can. J. Chem.* **1976**, *54*, 1643.
(26) Mayhew, C. A.; Peverall, R.; Timperley, C. M.; Watts, P. *Int. J. Mass Spectrom.* **2004**, *233*, 155.
(27) Staneke, P. O.; Groothuis, G.; Ingemann, S.; Nibbering, N. M. M. *Int. J. Mass Spectrom. Ion Processes* **1995**, *149*, 99.
(28) Staneke, P. O.; Groothuis, G.; Ingemann, S.; Nibbering, N. M. M. *J. Phys. Org. Chem.* **1996**, *9*, 471.
(29) Angel, L. A.; Ervin, K. M. *J. Am. Chem. Soc.* **2003**, *125*, 1014.
(30) Angel, L. A.; Ervin, K. M. *J. Phys. Chem. A* **2004**, *108*, 9827.
(31) Chen, H.; Cooks, R. G.; Meurer, E. C.; Eberlin, M. N. *J. Am. Soc. Mass Spectrom.* **2005**, *16*, 2045.
(32) Barlow, S. E.; Van Doren, J. M.; Bierbaum, V. M. *J. Am. Chem. Soc.* **1988**, *110*, 7240.
(33) Bunnett, J. F.; Garbisch, E. W.; Pruitt, K. M. *J. Am. Chem. Soc.* **1957**, *79*, 385.
(34) Bunnett, J. F. *Q. Rev. Chem. Soc.* **1958**, *12*, 1.
(35) Senger, N. A.; Bo, B.; Cheng, Q.; Keeffe, J. R.; Gronert, S.; Wu, W. *J. Org. Chem.* **2012**, *77*, 9535.
(36) Briscese, S. M.; Riveros, J. M. *J. Am. Chem. Soc.* **1975**, *97*, 230.
(37) Soukup, L. L.; Gronert, S. *Int. J. Mass Spectrom.* **2014**, in press.
(38) Glukhovtsev, M. N.; Pross, A.; Schlegel, H. B.; Bach, R. D.; Radom, L. *J. Am. Chem. Soc.* **1996**, *118*, 11258.
(39) Zhang, Y. *THEOCHEM* **2010**, *961*, 6.
(40) Li, T. H.; Wang, C. M.; Yu, S. W.; Xie, X. G. *Comput. Theor. Chem.* **2011**, *964*, 304.
(41) Bartmess, J. E. In *NIST Standard Reference Database Number 69*; Mallard, W. G., Linstrom, P. J., Eds.; National Institute of Standards and Technology: Gaithersburg, MD, 2014; http://webbook.nist.gov.
(42) Bierbaum, V. M. In *The Encyclopedia of Mass Spectrometry, Volume 1: Theory and Ion Chemistry*; Armentrout, P. B., Ed.; Elsevier: Amsterdam, 2003; pp 98−109.
(43) Van Doren, J. M.; Barlow, S. E.; DePuy, C. H.; Bierbaum, V. M. *Int. J. Mass Spectrom. Ion Processes* **1987**, *81*, 85.
(44) Su, T.; Bowers, M. T. In *Gas Phase Ion Chemistry*; Bowers, M. T., Ed.; Academic Press: New York, 1979; Vol. *1*, pp 83−118.
(45) Frisch, M. J. *Gaussian 03*; Gaussian, Inc.: Pittsburgh, PA, 2003.
(46) Scott, A. P.; Radom, L. *J. Phys. Chem.* **1996**, *100*, 16502.
(47) Freriks, I. L.; Dekoning, L. J.; Nibbering, N. M. M. *J. Am. Chem. Soc.* **1991**, *113*, 9119.